Published in final edited form as:
J Immunol. 2011 May 15; 186(10): 5603–5611. doi:10.4049/jimmunol.1003464.

Plexin-D1 Is a Novel Regulator of Germinal Centers and Humoral Immune Responses

Eda K. Holl[*,†], **Brian P. O'Connor**[‡], **T. Matt Holl**[§], **Kelly E. Roney**[*,†], **Albert G. Zimmermann**[*], **Sushmita Jha**[†], **Garnett Kelsoe**[§,1], and **Jenny P.-Y. Ting**[*,†,1]

[*]Department of Microbiology and Immunology, University of North Carolina, Chapel Hill, NC 27599

[†]Lineberger Comprehensive Cancer Center, University of North Carolina, Chapel Hill, NC 27599

[‡]Center for Genes, Environment, and Health, National Jewish Health, Denver, CO 80206

[§]Department of Immunology, Duke University, Durham, NC 27710

Abstract

Long-lived humoral immune responses depend upon the generation of memory B cells and long-lived plasma cells during the germinal center (GC) reaction. These memory compartments, characterized by class-switched IgG and high-affinity Abs, are the basis for successful vaccination. We report that a new member of the plexin family of molecules, plexin-D1, controls the GC reaction and is required for secondary humoral immune responses. Plexin-D1 was not required for B cell maturation, marginal zone precursor development, dark and light zone formation, Igλ^+ and Igκ^+ B cell skewing, B1/B2 development, and the initial extrafollicular response. Plexin-D1 expression was increased following B cell activation, and *PlxnD1*$^{-/-}$ mice exhibited defective GC reactions during T-dependent immune activation. *PlxnD1*$^{-/-}$ B cells showed a defect in migration toward the GC chemokines, CXCL12, CXCL13, and CCL19. Accordingly, *PlxnD1*$^{-/-}$ mice exhibited defective production of IgG1 and IgG2b, but not IgG3 serum Ab, accompanied by reductions in long-lived bone marrow plasmacytes and recall humoral memory responses. These data show a new role for immune plexins in the GC reaction and generation of immunologic memory.

Plexins were initially identified as molecules involved in axon guidance during neuronal development (1, 2). Emerging research on plexins has revealed that many of these family members are indispensable in developmental programs of the immune system (3) and are required for proper immune activation (4-8). Plexin-D1 was first shown to be important for its role in vasculature formation as well as heart development (9, 10), but recent work demonstrates its role in controlling migration of double-positive thymocytes (11). Plexins have different ligands by which they exert their function. The primary ligands for the plexin family of molecules are the semaphorins (3). Plexin-D1 has two known ligands, semaphorin-4A and semaphorin-3E (11, 12). However, semaphorin-3E is the only plexin-D1 ligand that has been identified in immune tissues (11).

Address correspondence and reprint requests to Dr. Jenny P.-Y. Ting, 450 West Drive, Lineberger Comprehensive Cancer Center, Room 209, Chapel Hill, NC 27599. jenny_ting@med.unc.edu.

[1]G.K. and J.P.-Y.T. contributed equally and should be considered cosenior authors.

The online version of this article contains supplemental material.

Disclosures

The authors have no financial conflicts of interest.

Successful activation of B cells during a T-dependent (T_d) immune response is essential in providing long-term immunity (13, 14). The T_d response results in follicular (FO) B cell activation and subsequent plasma cell development and germinal center (GC) formation (15). The initial T_d response results in low-affinity Ag-specific IgM or IgG production by short-lived plasma cells that reside in the spleen (16-18). The GC reaction, which develops more slowly, gives rise to memory B cells and long-lived bone marrow (BM) plasma cells that provide the rapid and robust serum Ab responses characteristic of secondary, memory responses (16, 19). GCs are the primary sites for affinity maturation, which is characterized by clonal expansion and somatic hypermutation (19).

Whereas many studies have addressed the GC response and the types of mechanisms involved in its initiation and maintenance, we lack a complete understanding of this process. Earlier work suggested that the GC is divided into two distinct compartments, the light and dark zone (20). The dark zone is characterized by rapidly proliferating B cells (centroblasts), which additionally undergo somatic hypermutation. The light zone is populated by FO dendritic cells that present Ag to activated B cells and facilitate clonal selection (21). This view has recently been revised as new data suggest that clonal selection can also occur in the dark zone (22). GC B cells found in the dark and light zones are not as morphologically different as originally thought (22, 23). Additionally, these studies report intrazonal circulation of GC B cells and substantial traffic along the GC periphery where B cells are thought to travel and receive T cell help (22, 23).

Previous studies have suggested that activated B cells specific for a foreign Ag seed the GC within a few days after the initiation of the immune response (13, 18, 24). B cells are then selected and continue on as long-lived plasma cells or memory B cells (22, 25, 26). Chemokines are key regulators of the GC reaction, as follows: the chemokine receptors such as CXCR4 and CXCR5 control formation and maintenance of GC (27-29); CXCL13 and its receptor CXCR5 direct activated B cells to the GC light zone and are required for proper positioning of the GC light zone (25); and CXCL12 is thought to be required for the recruitment of CXCR4-expressing GC B cells from the light zone into the dark zone (25). Although the identification of key chemokines and their receptors has furthered our understanding of the GC reaction, we still lack a complete picture of the molecular mechanisms involved in guiding B cells into and out of the GC reaction. Indeed, gene deletion studies focusing on CXCR4- and CXCR5-dependent mechanisms have suggested that GC formation is influenced by other, yet-to-be identified guidance molecules that traffic activated B cells in and out of the GC (22, 25, 26, 29).

A gene-profiling report found plexinB2 as one of the genes that are expressed by GC B cells, although the physiological relevance of this finding was not explored (30). Plexins and their receptors, semaphorins, play significant roles in cell migration and positioning in other immune organs and are, therefore, likely candidates to play important roles in formation and maintenance of the GC (3). Thus, it is important to explore the physiological and functional role of plexins in the GC reaction.

This work reveals that plexin-D1 is expressed by B lymphocytes and that expression is greatly enhanced in activated B cells. Moreover, *PlxnD1*$^{-/-}$ B cells fail to participate efficiently in the GC reaction. Additionally, recall immune responses are attenuated in the absence of plexin-D1 leading to defective Ab production. These results indicate a novel physiologic role of plexin-D1 in B cell activation.

Materials and Methods

Mice

C57BL/6 and congenic C57BL/6 CD45.1 mice were obtained from the National Cancer Institute (Boston, MA). *PlxnD1*$^{+/-}$ mice were a generous gift from Dr. Thomas Jessell's laboratory and have been described previously (9). Mice were housed in a pathogen-free barrier facility at University of North Carolina. These studies were approved by the University of North Carolina Animal Care and Use Committee.

For fetal liver chimeras, *PlxnD1*$^{+/-}$ mice were crossed for >10 generations with C57BL/6 mice and intercrossed to obtain *PlxnD1*$^{-/-}$ and *PlxnD1*$^{+/+}$ embryos. *PlxnD1*$^{+/+}$ and *PlxnD1*$^{-/-}$ fetal livers were prepared from E14 embryos post-PCR genotyping, as previously described (9). Five million fetal liver cells were then injected (i.v.) into lethally irradiated C57BL/6 CD45.1 mice. Mice were analyzed 6–10 wk postreconstitution. For mixed chimera experiments, fetal liver cells were obtained from *PlxnD1*$^{-/-}$ embryos (CD45.2) and *PlxnD1*$^{+/+}$ embryos (CD45.1), mixed (1:1 ratio), and injected into lethally irradiated C57BL/6 CD45.1 recipient mice. Mice were allowed to reconstitute for 6–8 wk before use.

Immunizations

4-Hydroxy-3-nitrophenylacetyl–chicken γ-globulin immunization—Fetal liver chimeric mice were immunized (i.p.) with 4-hydroxy-3-nitrophenylacetyl$_{18}$–chicken γ-globulin (NP$_{18}$-CGG; 10 μg) precipitated in alum and suspended in 200 μl PBS. Mice were bled before, 4 d, 7 d, 14 d, and 28 d after immunization to determine Ag-specific serum Ab levels. Spleens were harvested 4 d, 7 d, 14 d, and 21 d postimmunization and analyzed via FACS and immunofluorescent labeling of tissue sections. Remaining animals were boosted with NP$_{18}$-CGG (10 μg) at 28 d postprimary immunization. Serum was then collected 14 d postboost.

NP-Ficoll immunization—Fetal liver chimeric animals were immunized (i.p.) with NP-Ficoll (25 μg) suspended in 200 μl PBS. Mice were bled before, 3 d, and 5 d after immunization to determine Ag-specific serum Ab levels.

ELISA

ELISA plates (BD Falcon) were coated with 2 μg/ml (50 μl/well) capture reagent goat anti-mouse Ig$_{(H+L)}$, 4-hydroxy-3-nitroiodophenylacetyl (NIP)$_2$-BSA, or NIP$_{25}$-BSA in 0.1 M carbonate buffer (pH 9.5) overnight at 4°C. Detection Abs included HRP-conjugated goat anti-mouse IgM and goat anti-mouse IgG1, IgG2b, and IgG3 from Southern Biotechnology Associates (Birmingham, AL). Each serum sample was diluted 1:333 and was followed by 5–10 serial 3-fold dilutions and assayed in duplicate. Purified mouse IgM and IgG mAb were used to generate standard curves beginning at 1 μg/ml and diluted to 6 ng/ml.

In vitro B cell migration

FO (B220$^+$CD21^{low}CD23^{high}) B cells were sorted from the spleens of wild-type (WT) and *PlxnD1*$^{-/-}$ animals and activated in the presence of anti-μ and anti-CD40 overnight. Cells were then counted and suspended in RPMI 1640 with 0.1% fatty acid-free BSA. Cells were resuspended at a density of 10^7 cells/ml and incubated at 37°C for 30 min prior to Transwell migration assay. Media (100 μl) were added to the upper chamber of 24-well migration plates with a pore size of 5 μm (Corning Costar). Top chambers were inserted into wells containing 600 μl media with CCL19 (500 ng/ml), CXCL13 (500 ng/ml), or CXCL12 (150 ng/ml). Plates were incubated for 2 h at 37°C. All cells were counted by flow cytometry, as previously described (25).

ELISPOT assays

Ag-specific Ab-forming cells—ELISPOT plates (Millipore) were coated with 2 μg/ml (50 μl/well) NIP_{25}-BSA or goat anti-mouse $Ig_{(H+L)}$ in 0.1 M carbonate buffer (pH 9.5) overnight at 4°C. One million splenocytes (5 and 14 d postprimary immunization) and 1 million BM cells (14 d postboost) obtained from immunized animals were serially diluted and plated in triplicate. Cells were incubated at 37°C in a humidified CO_2 incubator for 4 h. Plates were washed and reblocked for 24 h using blocking buffer (1× PBS [pH 7.4], 0.1% Tween 20, and 0.5% BSA). Membranes were probed with alkaline phosphatase–conjugated IgG (Southern Biotechnology Associates), and spots were developed with Sigma *FAST* 5-bromo-4-chloro-3-indolyl phosphate/NBT (Sigma-Aldrich).

Cell culture

Proliferation assays—B cells were sorted by FACS or using a B cell-negative selection kit (StemCell Technologies). A total of 2×10^5 purified B cells was cultured in RPMI 1640 media (Life Technologies) containing 10% FBS, 10^{-4} M 2-ME, and penicillin/streptomycin antibiotics in 96-well plates. Cells were cultured in the presence of 5 μg/ml LPS (Sigma-Aldrich) or 5 μg/ml anti-μ (Jackson ImmunoResearch Laboratories) for 48 h. A total of 1 μCi [^{3}H]thymidine was added to the cultures for the last 8 h to assess proliferation. FACS-sorted FO ($B220^+CD21^{low}CD23^{high}$) B cells were labeled with 5 μM CFSE (Sigma-Aldrich) and cultured in the presence of 5 μg/ml IgM or 5 μg/ml LPS. Proliferation was assessed by flow cytometry after 72 h.

B cell activation—FO and marginal zone (MZ) B cells were sorted from the spleens of C57BL/6 animals and cultured in the presence of 5 μg/ml LPS (Sigma-Aldrich), 1 μg/ml anti-μ (Jackson ImmunoResearch Laboratories), or 1 μg/ml anti-CD40 (eBiosciences, San Diego, CA) for 72 h. RNA and cDNA for RT-PCR and quantitative real-time PCR were prepared, as described above.

Abs and FACS

mAbs included the following: B220 (RA3-6B2), CD23 (B3B4), BP1 (6C3), CD24 (M1/69), CD43 (S7), GL-7, and allophycocyanin Alexa750-conjugated streptavidin from BD Pharmingen (San Diego, CA); IgM (eB121-15F9), IgD (11-26), CD21 (eBio8D9), CD93 (AA4.1), CD5 (Ly-1), CD45.2 (104), CD4 (L3T4), CD8 (Ly-2), and TCRβ (H57-597) from eBiosciences; Igκ and Igλ from Southern Biotechnology Associates; and CD38 (90) and IgG1 (RMG1-1) from Biolegend (San Diego, CA). Secondary Abs included anti-FITC Alexa488, Alexa350-conjugated streptavidin, and Alexa405-conjugated streptavidin from Invitrogen (Raleigh, NC). Single-cell suspensions of different tissues were counted, and 10^6 cells were suspended in FACS buffer (1× PBS plus 2% FBS) and stained with various Ab combinations. All flow cytometry was performed on a FACSCalibur or LSRII cytometer (BD Biosciences) and analyzed with FlowJo software (Tree Star). Cell sorting was performed on a MoFlo cytometer (Beckman-Coulter).

Histology

Spleens from naive and immunized mice were embedded in OCT compound, snap frozen, and stored at −80°C. Sections (5 μm) were prepared and fixed with 1:1 acetone:methanol for 10 min at −20°C and labeled with various combinations of fluorescently labeled Abs. Additionally, sections from various spleens were H&E stained. Images were acquired using a Zeiss Axiovert 200M or Zeiss LSM 710 confocal immunofluorescent microscope.

Statistical analysis

Statistical significance was determined with two-tailed Student *t* test. All *p* values <0.05 were considered significant.

Results

PlxnD1 is predominantly expressed in B cells and upregulated by B cell activation

Expression of plexin-D1 in the immune system has not been fully characterized. *PlxnD1* was recently shown to be expressed by double-positive thymocytes and controlled movement within the thymus (11), indicating a role for *PlxnD1* in lymphocyte development and migration. We extended plexin-D1 expression studies from immature thymocytes to peripheral T and B cells using RT-PCR (Fig. 1*A*) and quantitative real-time PCR (Fig. 1*B*). *PlxnD1* mRNA expression is minimally detected in peripheral CD4 and CD8 T cells and in mature T cells that have been cultured under Th1 and Th2 skewing conditions. To characterize plexin-D1 expression in B cells, splenic (FO) ($B220^{+}IgD^{high}IgM^{low}CD21^{low}CD23^{high}$) and MZ ($B220^{+}IgD^{low}IgM^{high}CD21^{high}CD23^{low}$) B cells were isolated by flow cytometry. As shown by both RT-PCR and real-time PCR, *PlxnD1* mRNA was minimally expressed by resting naive FO B cells, slightly elevated in the GC B cell compartment, but highly expressed by MZ B cells (Fig. 1). Activation of sorted FO B cells with LPS, anti-IgM, and anti-CD40 resulted in dramatically increased (20- to 30-fold) plexin-D1 expression, suggesting that this gene might play a role in B cell immune responses (Fig. 1*B*). Thus, in peripheral lymphoid organs, plexin-D1 is constitutively expressed by MZ B cells and is upregulated in FO B cells upon activation. These data suggest that plexin-D1 expression is associated with activated B cell populations.

PlxnD1$^{-/-}$ B cells exhibit normal development and in vitro activation profiles in mice engrafted with PlxnD1$^{-/-}$ fetal liver cells

Conventional *plxnD1* gene inactivation in mice results in embryonic lethality, thereby prohibiting any study of a fully developed immune system (10). To determine whether the absence of plexin-D1 affects lymphocyte development, lethally irradiated C57BL/6 CD45.1 mice were reconstituted with either WT or *PlxnD1*$^{-/-}$ fetal liver cells. Donor and recipient hematopoietic cell populations were readily distinguished based on the expression of the CD45.1 (host) or CD45.2 (donor) allelic markers. Hematopoietic reconstitution of irradiated mice receiving either WT or *PlxnD1*$^{-/-}$ fetal liver was >90%, as assessed by flow cytometric analysis of splenocytes (Fig. 2*Ai*).

We analyzed B cell development in the BM of *PlxnD1*$^{-/-}$ and WT control mice by the criteria of Hardy, based on expression of B220, CD43, BP1, and heat stable Ag (HSA) (Fig. 2*Aii*, 2*Aiii*) (31). $B220^{+}CD43^{high}$ cells were separated into three populations, as follows: $BP1^{-}HSA^{-}$, $BP1^{-}HSA$, and $BP1^{+}HSA^{+}$: A (prepro-B cells), B (pro-B cells), and C (late pro-B cells). BM of *PlxnD1*$^{-/-}$ and WT control animals showed no difference in the percentage of pro-B cells and pre-B cells (Fig. 2*Aiii*). These data demonstrate that expression of plexin-D1 is not required to generate early progenitor B cell compartments.

To evaluate B cell development and maturation, we examined the splenic B cell compartments of *PlxnD1*$^{-/-}$ and WT control animals using mAbs to B220, IgM, IgD, CD21, CD23, and CD93. The immature transitional B cell compartments, defined by IgM, CD23, and CD93 expression (32), were similar in *PlxnD1*$^{-/-}$ and WT animals, suggesting that B cell development in the spleen is normal (Supplemental Fig. 1*A*). FO B cell ($IgM^{int}IgD^{high}$) frequencies were also comparable between *PlxnD1*$^{-/-}$ and WT control animals (Fig. 2*Aiv*). In contrast, when MZ B cells were examined, there was a 2-fold reduction in the percentage of these cells in *PlxnD1*$^{-/-}$ mice compared with WT controls, whereas FO B cell

percentages remained unchanged, thus suggesting a potential importance of plexin-D1 in MZ function (Fig. 2*B*). All data, including total cell numbers, are compiled in Supplemental Table 1. In addition, we examined the B cell compartment in the peritoneal cavity of *PlxnD1*$^{-/-}$ animals and no differences were found in the percentages and numbers of B1 and B2 compartments (Supplemental Fig. 1*B*).

The proliferation of *PlxnD1*$^{-/-}$ B cells in response to anti-IgM or LPS stimulation as determined by [^{3}H]thymidine incorporation (Fig. 2*C*) or CFSE dilution (Fig. 2*D*) was normal in *PlxnD1*$^{-/-}$ FO and MZ B cells. Histological studies of the spleen revealed normal splenic architecture in *PlxnD1*$^{-/-}$ mice, as determined by characteristic white and red pulp structure (Fig. 2*E*). These data suggest that plexin-D1 is dispensable for B cell proper localization in the spleen.

PlxnD1$^{-/-}$ animals have attenuated GC responses

The reduction in the percentage of MZ B cells in *PlxnD1*$^{-/-}$ animals compared with WT led us to investigate whether humoral immune responses were affected by the absence of plexin-D1. We analyzed basal Ig levels in WT and *PlxnD1*$^{-/-}$ sera by ELISA. Basal total IgM and IgG3 were comparable between WT and *PlxnD1*$^{-/-}$ animals, but IgG1 and IgG2b levels were significantly reduced in *PlxnD1*$^{-/-}$ mice compared with WT mice (Fig. 2*F*).

The defect in T_d Ig class switching could be attributed to impaired GC reactions in *PlxnD1*$^{-/-}$ animals. GCs are pivotal sites for facilitating Ig class switching, and we analyzed, therefore, the formation of GCs in the spleens of *PlxnD1*$^{-/-}$ and control mice after NP-CGG immunization (15). Spleens were harvested on day 14 postimmunization, and splenocytes were analyzed by flow cytometry to determine the frequency of B220^{high}GL-7^{high} GC B cells (29) present within the total B220^{+} population. Whereas there was no difference at naive state, *PlxnD1*$^{-/-}$ animals showed a lower percentage of GC B cells when compared with WT postimmunization (Fig. 3*A*). We observed a 2-fold reduction in the percentage and numbers of GC B cells for *PlxnD1*$^{-/-}$ mice, at days 7, 14, and 21, compared with WT ($p < 0.01$) (Fig. 3*B*, Supplemental Table 1). There was no significant difference in the percentages of B220^{high}GL-7^{+} B cells between WT and *PlxnD1*$^{-/-}$ mice at day 4, suggesting that the kinetics of GC onset were not changed by plexin-D1 (Fig. 3*B*). Splenic cryosections were labeled with mAbs to TCRβ, B220, and GL-7 to determine whether GCs form in *PlxnD1*$^{-/-}$ mice. *PlxnD1*$^{-/-}$ animals showed a reduction in the size of the GCs as determined by histology at day 14 (Fig. 3*C*). B cell contribution to GC formation was entirely of donor origin (Supplemental Fig. 2*A*). Additionally, we stained splenic sections with CD21 to determine the dark and light zone of the GCs in WT and *PlxnD1*$^{-/-}$ animals (Supplemental Fig. 2*B*). Our data demonstrate that dark and light zones are present in both WT and *PlxnD1*$^{-/-}$ mice despite the size of the GCs.

To expand the analysis of GC frequency in WT and *PlxnD1*$^{-/-}$ mice, five to eight nonserial sections were prepared from immunized spleen samples. The number of GCs was counted and normalized to the number of follicles per section to account for differences in area. These results showed that the number of follicles that contained GCs was lower in the *PlxnD1*$^{-/-}$ animals compared with WT controls (Fig. 4*A*). To quantify the difference in GC size between *PlxnD1*$^{-/-}$ and WT animals, the area of individual GCs was measured using ImageJ software. Whereas WT animals showed a higher distribution of the medium and large GCs, *PlxnD1*$^{-/-}$ mice contained an elevated frequency of small GCs and a reduced frequency of large GCs (Fig. 4*B*). A compilation of >200 GC/mouse type shows that the size of GCs in *PlxnD1*$^{-/-}$ mice is reduced by ~2-fold compared with the WT controls (Fig. 4*C*). Taken together, these data demonstrate that hematopoietic-derived plexin-D1 controls both the number and size of GCs formed during immunization.

The NP-hapten elicits a restricted Ab response to $Igh^b/\lambda 1$ mice (33). To exclude the possibility that the differences we observed in the GC reaction are a result of different frequencies of $Ig\lambda^+$ B cells in the absence of plexin-D1, we enumerated $Ig\lambda^+$ B cells in *PlxnD1*$^{-/-}$ mice and found comparable percentages and distributions of $Ig\lambda^+$ B cells to WT (Supplemental Fig. 3*A*, 3*B*). We also determined the presence of $Ig\lambda^+$ cells in the GCs of WT and *PlxnD1*$^{-/-}$ mice (Supplemental Fig. 3*C*).

PlxnD1$^{-/-}$ B cells participate in the GC reaction less efficiently than WT B cells

To determine whether the expression of plexin-D1 was required for optimal GC formation, irradiated WT mice were reconstituted with fetal liver cells from *PlxnD1*$^{-/-}$ and WT mice (Fig. 5*A*). After 8 wk, double chimera mice were immunized with NP-CGG. Fourteen days after immunization, spleens from immunized and naive mice were analyzed by flow cytometry and histology. The reconstitution of irradiated recipients by WT and *PlxnD1*$^{-/-}$ B cells was similar (Fig. 5*B*). We determined the frequency of GC B cells ($B220^{high}GL\text{-}7^{high}$) in the chimeric mice postimmunization. Flow cytometry analysis revealed a near 3-fold decrease in the percentage of GC B cells derived from *PlxnD1*$^{-/-}$ fetal liver cells compared with WT (Fig. 5*B*, 5*C*). Results obtained from six individual mice are compiled in Fig. 5*C*. Additionally, we performed immunofluorescence staining on sections obtained from the spleens of chimeric mice to determine the presence of WT or *PlxnD1*$^{-/-}$ B cells in the GC (Fig. 5*Di*). We observed a lack of $CD45.2^+$ *PlxnD1*$^{-/-}$ B cells in >70% of the GC examined. In a competitive environment, *PlxnD1*$^{-/-}$ B cells are less efficient than WT cells in entering GC. Additionally, we stained splenic sections with CD21 to define the light zone of the GC. We observed abundant $CD45.1^+$ WT, but only occasional $CD45.2^+$ *PlxnD1*$^{-/-}$ B cells in the light zone of the GCs (Fig. 5*Dii*). The majority of *PlxnD1*$^{-/-}$ B cells accumulated around the GCs. These data are consistent with the results obtained earlier with *PlxnD1*$^{-/-}$ mice to indicate that formation of GC is impaired.

PlxnD1$^{-/-}$ B cells exhibit reduced migration to CXCL12, CXCL13, or CCL19

To investigate possible mechanisms behind the reduced size and frequency of GC in *PlxnD1*$^{-/-}$ mice, the response to B cell chemokines involved in GC recruitment (CXCL12, CXCL13, and CCL19) was measured using an in vitro Transwell migration assay performed with naive and activated B cells.

In addition to the in vivo experiment described in Fig. 5 in which WT and *PlxnD1*$^{-/-}$ B cells were assessed for their participation in the GC in a competitive assay, we performed an analogous experiment in which naive or activated WT and *PlxnD1*$^{-/-}$ B cells were combined in an in vitro competitive B cell migration assay toward CXCL12, CXCL13, and CCL19. Migration of B cells was quantified by flow cytometry, and data are presented as the percentage of migrating B cells over input. Migration of naive B cells toward these chemokines was not affected (Supplemental Fig. 4*A*). However, migration of activated B cells was uniformly reduced in *PlxnD1*$^{-/-}$ cells compared with WT B cells in the same wells (Fig. 6*A*). We also assessed the cell surface expression of receptors for CCL19, CXCL12, and CXCL13 by flow cytometry. We did not observe significant differences in cell surface expression for CCR7, CXCR4, and CXCR5 in naive or activated B cells (data not shown), indicating that the lack of responsiveness to chemokines was not due to lowered expression of the associated chemokine receptors. These observations demonstrate that plexin-D1 regulates B cell migratory responses to a panel of chemokines important for GC reaction. Additionally, we assessed T cell migration in vitro in response to CXCL12 and CCL19 chemokines. T cell migration was not affected in the absence of plexin-D1 as compared with WT mice (Supplemental Fig. 4*B*).

To determine whether the loss of GC B cells in the absence of plexin-D1 was associated with altered GC B cell proliferation, we quantified the percentages of proliferating GC B cells by BrdU incorporation at day 14 postimmunization. As shown in Fig. 6*B*, absence of plexin-D1 does not affect the proliferation rate of GC B cells. Similarly, BrdU incorporation in non-GC B cells is comparable between *PlxnD1*$^{-/-}$ and WT animals (Supplemental Fig. 5). Additionally, we determined whether diminished GC B cells were due to increased B cell death in the absence of plexin-D1. To this end, we employed TUNEL staining. As shown in Fig. 6*C*, the numbers of TUNEL^{+} cells were comparable between WT and *PlxnD1*$^{-/-}$ GCs. Together, these data suggest that decreased numbers of GC B cells in the absence of plexin-D1 are not due to diminished in vivo B cell proliferation or increased B cell death. We attribute the decreased ability of *PlxnD1*$^{-/-}$ animals to form robust GCs to the inability of B cells to efficiently migrate into the GCs in the absence of plexin-D1.

PlxnD1$^{-/-}$ mice show attenuated secondary humoral immune response

Given the impaired GC response of *PlxnD1*$^{-/-}$ chimeras, we examined the generation of humoral immune memory in these mice. The GC reaction is crucial for the efficient production of memory B cells and long-lived BM plasma cells, which comprise the cellular memory compartments (16, 19). To measure memory B cell responses, WT and *PlxnD1*$^{-/-}$ mice were immunized with NP-CGG in alum and then boosted with NP-CGG 28 d postprimary immunization. Serum samples were collected before immunization, 7 d, 14 d, and 28 d postprimary immunization, and 14 d after secondary boost. An ELISA to determine both total- and high-affinity serum Ab was performed with all serum samples.

Naive *PlxnD1*$^{-/-}$ or WT mice contained low to undetectable levels of NP-reactive IgG1 Ab, whereas 14 d postimmunization NP-specific Ab levels in these mice increased (~1000-fold) (Fig. 7*A*). Primary serum Ab responses of *PlxnD1*$^{-/-}$ and WT animals did not differ ($p > 0.05$) in high- or total-affinity Ab levels (Fig. 7*A*, 7*B*). Secondary Ab responses, however, were significantly reduced ($p < 0.05$) in *PlxnD1*$^{-/-}$ mice compared with WT for both low- and high-affinity Ab (Fig. 7*A*, 7*B*). These results showed that the initial immune response in *PlxnD1*$^{-/-}$ mice is similar to WT controls, whereas a secondary challenge revealed that the recall response is suboptimal in *PlxnD1*$^{-/-}$ mice. To determine the effect of plexin-D1 in affinity maturation, we obtained the ratio of NP2/NP25 (Fig. 7*C*).

To examine whether Ag-specific class switching Ab-forming cells (AFC) were affected in *PlxnD1*$^{-/-}$ animals, we performed ELISPOT assays to determine the frequencies of NP-specific IgG-secreting cells in the spleens of immunized mice at 5 and 14 d after primary immunization. The number of splenic NP-specific AFC increased after immunization compared with naive controls in both WT and *PlxnD1*$^{-/-}$ animals. However, the frequency of NP-specific IgG AFC was lower in *PlxnD1*$^{-/-}$ animals compared with WT animals at day 14, but not at day 5 after primary immunization (Fig. 7*D*). Interestingly, we did not observe a difference in the numbers of NP-specific IgM AFC at day 5 and 14 postimmunization, suggesting that formation of nonclass-switched plasma cells is normal in *PlxnD1*$^{-/-}$ animals (Supplemental Fig. 6). Taken together, these data suggest that initial extrafollicular responses in *PlxnD1*$^{-/-}$ mice are intact. We also compared the levels of NP-specific AFC in the BM of *PlxnD1*$^{-/-}$ or WT control animals following a secondary boost where long-lived, memory AFC reside. *PlxnD1*$^{-/-}$ mice exhibited a reduction of NP-specific IgG AFC following secondary challenge (Fig. 7*E*). We correlate a reduction in the frequency of NP-specific AFC with reduced levels of IgG1 observed at day 42, which is 14 d after the secondary challenge.

Taken together, these data suggest that although initial AFC formation is normal in *PlxnD1*$^{-/-}$ mice, the continued generation of these cells is reduced as compared with WT controls.

We also examined the role of plexin-D1 during a T-independent immune response by immunizing *PlxnD1*$^{-/-}$ and WT mice with NP-Ficoll in PBS. There were no significant differences in the levels of NP-specific serum IgM between WT and *PlxnD1*$^{-/-}$ mice in response to NP-Ficoll (Supplemental Fig. 7). Thus, plexin-D1 expression on B cells appears to specifically regulate GCs and the formation of humoral immune memory associated with T_d responses.

Discussion

This study identifies a novel role for plexin-D1 in B cell biology and, to our knowledge, represents the first demonstration of a plexin molecule that affects GC formation and humoral immune memory. In our study, *PlxnD1* was expressed at low levels by FO B cells and substantially induced by LPS, IgM, or CD40 engagement. Despite its relative abundance in activated B cells, plexin-D1 was not required for FO B cell development and maturation as all B cell subpopulations tested were present in normal frequencies in the BM, spleen, peritoneal cavity, and lymph nodes of *PlxnD1*$^{-/-}$ animals.

The enhancement of *PlxnD1* expression by B cells following activation suggested a role for this molecule during the course of an immune response. Indeed, immunization with T_d Ags resulted in a reduced memory IgG1 response in *PlxnD1*$^{-/-}$ mice compared with the WT mice, accompanied by reduced size and numbers of splenic GCs. The GC is a primary site for class switch recombination, affinity maturation, and plasma cell and memory cell development (13, 18, 29). The reduced frequency of GC B cells was followed by a significant reduction in Ag-specific AFC formation in the BM following secondary challenge. The size and frequency of GCs are important in providing a pool of B cells that develop into AFC-producing class-switched Ab (29). Plexin-D1 is important in controlling these events and, thereby, ensures robust humoral responses. Additionally, Plexin-D1 may be important in specifically regulating either the generation or maintenance of memory B cells. Both of these events are needed to provide a robust memory immune response, and defects in either compartment can result in ablated Ab responses (17, 21).

Defects in the GC reaction can be the result of abnormal structural organization of lymphoid tissues (34). For example, *LTα*$^{-/-}$ mice have disturbed splenic architecture due to the inability of T and B cells to form distinct T and B cell zones (35). This phenomenon leads to unsuccessful IgG responses in these mice following immunization (35). Immunohistochemistry analysis of *PlxnD1*$^{-/-}$ spleens revealed normal splenic architecture, suggesting that the separation of B and T cells into distinct compartments is unaffected in these animals. Moreover, these data suggest that homing of B and T cells into secondary lymphoid organs is intact in the absence of plexin-D1.

Early T-independent immune responses in *PlxnD1*$^{-/-}$ animals are not affected, in the context of the NP-Ficoll response, despite a reduction in the number of MZ B cells. This suggests differential requirements for plexin-D1 during the course of an in vivo immune response controlled by different B cell subtypes. These data resemble the phenotype observed in *Rap1b*$^{-/-}$ animals in which the MZ B cell compartment is reduced due to the role of *rap1b* in controlling integrin functions (36). However, *Rap1b*$^{-/-}$ mice exhibit unaltered FO B cell compartments. MZ B cells can participate in the T_d immune response by acting as APCs and shuttling in and out of the follicles (37). A reduction in MZ B cell numbers can result in altered T_d responses. However, assessment of early T_d responses in *PlxnD1*$^{-/-}$ mice suggests that the phenotype observed in the absence of plexin-D1 is probably not due to the reduced numbers of MZ B cells.

Plexins were originally identified in the nervous system as receptors for semaphorins, a large class of both secreted and membrane-bound glycoproteins (38). Plexins are grouped into four different families (A, B, C, and D) based on their structural homology (38). Semaphorins are divided into eight subclasses, as follows: classes 1 and 2 belong to invertebrates, classes 3–7 belong to vertebrates, and class 8 belongs to viruses. Semaphorins can bind to their primary receptors, plexins, alone, or in the presence of neuropilin receptors. Plexins control cell adhesion via their intracellular domains, which contain GTPase-binding structures and are responsible for an array of signaling cascades (39, 40). Absence of plexins can lead to impaired immune responses controlled by various cell types (4-8).

The importance of plexin-D1 in cell adhesion and migration has been demonstrated in both the vascular and immune system. Absence of plexin-D1 results in aberrant vasculature patterning and growth via mechanisms that involve R-Ras and Arf6 (9, 40). In the immune system, absence of plexin-D1 results in impaired activated thymocyte migration toward CXCL12 and CCL23 chemokines (11). We extend these studies to show a role for plexin-D1 in B cell movement in peripheral lymphoid organs. In vivo, lack of plexin-D1 results in impaired B cell movement and participation in the GC. In vitro, migration of plexin-D1–deficient B cells toward chemokines that are implicated in T_d immune responses as well as the GC reaction is impaired. CCL19 has been implicated in recruiting B cells to the spleen and further contributing to their ability to travel and scan different areas in search for their cognate Ag (41, 42). Additionally, CXCL13 is highly expressed in the spleen and is required for migration of B cells to the follicles and subsequently to nascent GCs (25, 28). CCL19, CXCL12, and CXCL13 are thought to be important in setting up GCs and additionally regulating recruitment of B cells to the light and dark zones (25). Our in vitro migration experiments revealed that activated B cells had a reduction in migration abilities toward the tested chemokines, CXCL12, CXCL13, and CCL19. This occurred despite the fact that the receptors for these chemokines were expressed at normal levels by *PlxnD1*$^{-/-}$ B cells. These findings suggest that plexin-D1 may be important in allowing activated B cells to enter the GC in vivo by facilitating effective migration toward GC chemokines. Upregulation of plexin-D1 expression by activated B cells may be an important mechanism that initiates activated B cell movement and prompts Ag-specific B cells to participate in the GC reaction. Once this process is initiated, GC B cells downregulate plexin-D1 perhaps as a mechanism to facilitate their retention in the GC. We have identified a novel mechanism regulating B cell migration to GC chemokines that is distinct from chemokine receptor expression. The stage at which the defect in the GC response occurs needs to be established. It is possible that this defect occurs prior to the initiation of the GC reaction and absence of plexin-D1 in activated B cells blocks participation of activated B cells in the GC response. Moreover, the mechanisms underlying the ability of plexin-D1 to specifically regulate migration of GC B cells to CXCL12, CXCL13, and CCL19 will be examined in future studies.

The importance of plexins and semaphorins in controlling immune cell development and immune responses is recently being appreciated. For example, Plexin-B1 is required for proliferation and survival of B cells (4). Plexin-A1 expression by DCs is needed for proper T cell activation and proliferation via control of rho activation and actin polarization events in DCs (8, 43). Plexin-A4 is a negative regulator of T cell immune responses, and its absence leads to development of autoimmunity in mice lacking plexin-A4 (5). Most recently, expression of plexin-B2 in B cells was used to identify GCs (30). In this study, we have identified plexin-D1 as a novel regulator of humoral immune memory. Some of the defects observed over the course of T_d immune responses could be attributed to the inability of activated *PlxnD1*$^{-/-}$ B cells to migrate to the GC. These studies show that a single member of the plexin family can exert various functions on different cell types (T and B) depending on the stage of cell development or the state of immune activation. Further studies involving *PlxnD1*$^{-/-}$ T cells and B cells are needed to define the role of this

molecule in different types of immune responses. Plexin-D1 is, to our knowledge, the first plexin shown to be directly involved in the control of GCs and consequently control of humoral immune memory. This finding has implications in vaccine design in terms of targeting the GC and promoting long-term immunity.

Supplementary Material

Refer to Web version on PubMed Central for supplementary material.

Acknowledgments

We thank Dr. Robert Bagnell at the Microscopy Services Laboratory for assistance with microscopy.

This work was supported by University of North Carolina Developmental Biology Training Program Grant HD046369 (to E.K.H.), National Institutes of Health Grant AI29564 (to J.P.-Y.T.), National Institutes of Health Grant AI024335 (to G.K.), National Institutes of Health T32 Training Grant AI007151 (to A.G.Z.), National Institutes of Health T32 Lineberger Postdoctoral Training Grant (to B.P.O.), National Institutes of Health F32 Postdoctoral Grant (to B.P.O.), and an Irvington Institute Postdoctoral Fellowship from the Cancer Research Institute (to B.P.O.).

References

1. Winberg ML, Noordermeer JN, Tamagnone L, Comoglio PM, Spriggs MK, Tessier-Lavigne M, Goodman CS. Plexin A is a neuronal semaphorin receptor that controls axon guidance. Cell. 1998; 95:903–916. [PubMed: 9875845]
2. Kolodkin AL, Matthes DJ, Goodman CS. The semaphorin genes encode a family of transmembrane and secreted growth cone guidance molecules. Cell. 1993; 75:1389–1399. [PubMed: 8269517]
3. Suzuki K, Kumanogoh A, Kikutani H. Semaphorins and their receptors in immune cell interactions. Nat Immunol. 2008; 9:17–23. [PubMed: 18087252]
4. Granziero L, Circosta P, Scielzo C, Frisaldi E, Stella S, Geuna M, Giordano S, Ghia P, Caligaris-Cappio F. CD100/Plexin-B1 interactions sustain proliferation and survival of normal and leukemic CD5+ B lymphocytes. Blood. 2003; 101:1962–1969. [PubMed: 12406905]
5. Yamamoto M, Suzuki K, Okuno T, Ogata T, Takegahara N, Takamatsu H, Mizui M, Taniguchi M, Chédotal A, Suto F, et al. Plexin-A4 negatively regulates T lymphocyte responses. Int Immunol. 2008; 20:413–420. [PubMed: 18209113]
6. Walzer T, Galibert L, De Smedt T. Dendritic cell function in mice lacking Plexin C1. Int Immunol. 2005; 17:943–950. [PubMed: 15967782]
7. O'Connor BP, Eun SY, Ye Z, Zozulya AL, Lich JD, Moore CB, Iocca HA, Roney KE, Holl EK, Wu QP, et al. Semaphorin 6D regulates the late phase of CD4+ T cell primary immune responses. Proc Natl Acad Sci USA. 2008; 105:13015–13020. [PubMed: 18728195]
8. Wong AW, Brickey WJ, Taxman DJ, van Deventer HW, Reed W, Gao JX, Zheng P, Liu Y, Li P, Blum JS, et al. CIITA-regulated plexin-A1 affects T-cell-dendritic cell interactions. Nat Immunol. 2003; 4:891–898. [PubMed: 12910265]
9. Gu C, Yoshida Y, Livet J, Reimert DV, Mann F, Merte J, Henderson CE, Jessell TM, Kolodkin AL, Ginty DD. Semaphorin 3E and plexin-D1 control vascular pattern independently of neuropilins. Science. 2005; 307:265–268. [PubMed: 15550623]
10. Gitler AD, Lu MM, Epstein JA. PlexinD1 and semaphorin signaling are required in endothelial cells for cardiovascular development. Dev Cell. 2004; 7:107–116. [PubMed: 15239958]
11. Choi YI, Duke-Cohan JS, Ahmed WB, Handley MA, Mann F, Epstein JA, Clayton LK, Reinherz EL. PlexinD1 glycoprotein controls migration of positively selected thymocytes into the medulla. Immunity. 2008; 29:888–898. [PubMed: 19027330]
12. Chauvet S, Cohen S, Yoshida Y, Fekrane L, Livet J, Gayet O, Segu L, Buhot MC, Jessell TM, Henderson CE, Mann F. Gating of Sema3E/PlexinD1 signaling by neuropilin-1 switches axonal repulsion to attraction during brain development. Neuron. 2007; 56:807–822. [PubMed: 18054858]

13. Jacob J, Kassir R, Kelsoe G. In situ studies of the primary immune response to (4-hydroxy-3-nitrophenyl)acetyl. I. The architecture and dynamics of responding cell populations. J Exp Med. 1991; 173:1165–1175. [PubMed: 1902502]
14. Blink EJ, Light A, Kallies A, Nutt SL, Hodgkin PD, Tarlinton DM. Early appearance of germinal center-derived memory B cells and plasma cells in blood after primary immunization. J Exp Med. 2005; 201:545–554. [PubMed: 15710653]
15. Jacob J, Kelsoe G. In situ studies of the primary immune response to (4-hydroxy-3-nitrophenyl)acetyl. II. A common clonal origin for periarteriolar lymphoid sheath-associated foci and germinal centers. J Exp Med. 1992; 176:679–687. [PubMed: 1512536]
16. Allen CD, Okada T, Cyster JG. Germinal-center organization and cellular dynamics. Immunity. 2007; 27:190–202. [PubMed: 17723214]
17. Jacob J, Kelsoe G, Rajewsky K, Weiss U. Intraclonal generation of antibody mutants in germinal centres. Nature. 1991; 354:389–392. [PubMed: 1956400]
18. Liu YJ, Zhang J, Lane PJ, Chan EY, MacLennan IC. Sites of specific B cell activation in primary and secondary responses to T cell-dependent and T cell-independent antigens. Eur J Immunol. 1991; 21:2951–2962. [PubMed: 1748148]
19. Jacob J, Przylepa J, Miller C, Kelsoe G. In situ studies of the primary immune response to (4-hydroxy-3-nitrophenyl)acetyl. III. The kinetics of V region mutation and selection in germinal center B cells. J Exp Med. 1993; 178:1293–1307. [PubMed: 8376935]
20. Close PM, Pringle JH, Ruprai AK, West KP, Lauder I. Zonal distribution of immunoglobulin-synthesizing cells within the germinal centre: an in situ hybridization and immunohistochemical study. J Pathol. 1990; 162:209–216. [PubMed: 2125071]
21. Kelsoe G. Life and death in germinal centers (redux). Immunity. 1996; 4:107–111. [PubMed: 8624801]
22. Hauser AE, Junt T, Mempel TR, Sneddon MW, Kleinstein SH, Henrickson SE, von Andrian UH, Shlomchik MJ, Haberman AM. Definition of germinal-center B cell migration in vivo reveals predominant intrazonal circulation patterns. Immunity. 2007; 26:655–667. [PubMed: 17509908]
23. Allen CD, Okada T, Tang HL, Cyster JG. Imaging of germinal center selection events during affinity maturation. Science. 2007; 315:528–531. [PubMed: 17185562]
24. Wang Y, Carter RH. CD19 regulates B cell maturation, proliferation, and positive selection in the FDC zone of murine splenic germinal centers. Immunity. 2005; 22:749–761. [PubMed: 15963789]
25. Allen CD, Ansel KM, Low C, Lesley R, Tamamura H, Fujii N, Cyster JG. Germinal center dark and light zone organization is mediated by CXCR4 and CXCR5. Nat Immunol. 2004; 5:943–952. [PubMed: 15300245]
26. Schwickert TA, Lindquist RL, Shakhar G, Livshits G, Skokos D, Kosco-Vilbois MH, Dustin ML, Nussenzweig MC. In vivo imaging of germinal centres reveals a dynamic open structure. Nature. 2007; 446:83–87. [PubMed: 17268470]
27. Freedman AS, Munro JM, Rice GE, Bevilacqua MP, Morimoto C, McIntyre BW, Rhynhart K, Pober JS, Nadler LM. Adhesion of human B cells to germinal centers in vitro involves VLA-4 and INCAM-110. Science. 1990; 249:1030–1033. [PubMed: 1697696]
28. Förster R, Mattis AE, Kremmer E, Wolf E, Brem G, Lipp M. A putative chemokine receptor, BLR1, directs B cell migration to defined lymphoid organs and specific anatomic compartments of the spleen. Cell. 1996; 87:1037–1047. [PubMed: 8978608]
29. Arnold CN, Campbell DJ, Lipp M, Butcher EC. The germinal center response is impaired in the absence of T cell-expressed CXCR5. Eur J Immunology. 2007; 37:100–109. [PubMed: 17171760]
30. Yu D, Cook MC, Shin DM, Silva DG, Marshall J, Toellner KM, Havran WL, Caroni P, Cooke MP, Morse HC, et al. Axon growth and guidance genes identify T-dependent germinal centre B cells. Immunol Cell Biol. 2008; 86:3–14. [PubMed: 17938642]
31. Li YS, Wasserman R, Hayakawa K, Hardy RR. Identification of the earliest B lineage stage in mouse bone marrow. Immunity. 1996; 5:527–535. [PubMed: 8986713]
32. Wilker PR, Kohyama M, Sandau MM, Albring JC, Nakagawa O, Schwarz JJ, Murphy KM. Transcription factor Mef2c is required for B cell proliferation and survival after antigen receptor stimulation. Nat Immunol. 2008; 9:603–612. [PubMed: 18438409]

33. Rajewsky K. Clonal selection and learning in the antibody system. Nature. 1996; 381:751–758. [PubMed: 8657279]
34. Matsumoto M, Lo SF, Carruthers CJ, Min J, Mariathasan S, Huang G, Plas DR, Martin SM, Geha RS, Nahm MH, Chaplin DD. Affinity maturation without germinal centres in lymphotoxin-alpha-deficient mice. Nature. 1996; 382:462–466. [PubMed: 8684487]
35. De Togni P, Goellner J, Ruddle NH, Streeter PR, Fick A, Mariathasan S, Smith SC, Carlson R, Shornick LP, Strauss-Schoenberger J, et al. Abnormal development of peripheral lymphoid organs in mice deficient in lymphotoxin. Science. 1994; 264:703–707. [PubMed: 8171322]
36. Chen Y, Yu M, Podd A, Wen R, Chrzanowska-Wodnicka M, White GC, Wang D. A critical role of Rap1b in B-cell trafficking and marginal zone B-cell development. Blood. 2008; 111:4627–4636. [PubMed: 18319399]
37. Martin F, Kearney JF. Marginal-zone B cells. Nat Rev Immunol. 2002; 2:323–335. [PubMed: 12033738]
38. Kruger RP, Aurandt J, Guan KL. Semaphorins command cells to move. Nat Rev Mol Cell Biol. 2005; 6:789–800. [PubMed: 16314868]
39. Oinuma I, Ishikawa Y, Katoh H, Negishi M. The Semaphorin 4D receptor Plexin-B1 is a GTPase activating protein for R-Ras. Science. 2004; 305:862–865. [PubMed: 15297673]
40. Sakurai A, Gavard J, Annas-Linhares Y, Basile JR, Amornphimoltham P, Palmby TR, Yagi H, Zhang F, Randazzo PA, Li X, Weigert R, Gutkind JS, et al. Semaphorin 3E initiates anti-angiogenic signaling through Plexin-D1 by regulating Arf6 and R-Ras. Mol Cell Biol.
41. Okada T, Miller MJ, Parker I, Krummel MF, Neighbors M, Hartley SB, O'Garra A, Cahalan MD, Cyster JG. Antigen-engaged B cells undergo chemotaxis toward the T zone and form motile conjugates with helper T cells. PLoS Biol. 2005; 3:e150. [PubMed: 15857154]
42. Okada T, Ngo VN, Ekland EH, Förster R, Lipp M, Littman DR, Cyster JG. Chemokine requirements for B cell entry to lymph nodes and Peyer's patches. J Exp Med. 2002; 196:65–75. [PubMed: 12093871]
43. Eun SY, O'Connor BP, Wong AW, van Deventer HW, Taxman DJ, Reed W, Li P, Blum JS, McKinnon KP, Ting JP. Cutting edge: rho activation and actin polarization are dependent on plexin-A1 in dendritic cells. J Immunol. 2006; 177:4271–4275. [PubMed: 16982860]

Abbreviations used in this article

AFC	Ab-forming cell
BM	bone marrow
CGG	chicken γ-globulin
FO	follicular
GC	germinal center
HSA	heat stable Ag
MZ	marginal zone
NIP	4-hydroxy-3-nitroiodophenylacetyl
NP	4-hydroxy-3-nitrophenylacetyl
T_d	T-dependent
WT	wild-type

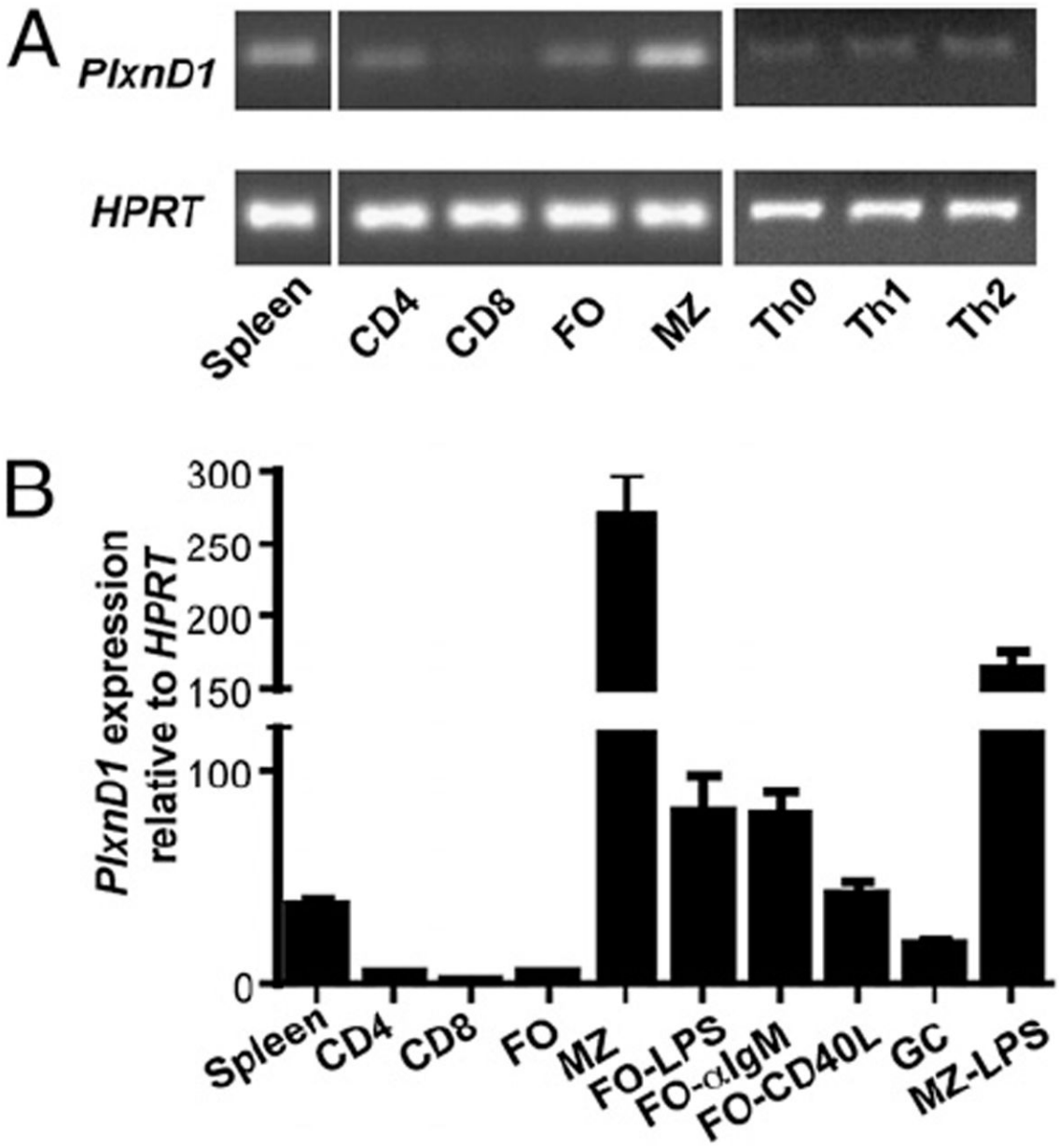

FIGURE 1.

Expression of plexin-D1 by lymphocytes. *A*, Expression of *PlxnD1* in the spleen, resting CD4 and CD8 T cells, MZ and FO B cells, and Th1 and Th2 cells, assessed by RT-PCR. Data are representative of three independent experiments. *B*, Expression of *PlxnD1* in sorted resting T cells; FO, GC, and MZ B cells; and activated B cells, as assessed by real-time PCR. All values were normalized to *HPRT*. B cells were cultured in the presence of LPS (5 μg/ml), anti-μ (1 μg/ml), or anti-CD40 (1 μg/ml) for 72 h. Data are representative of three independent experiments. Mean ± SEM. $n = 8$ mice.

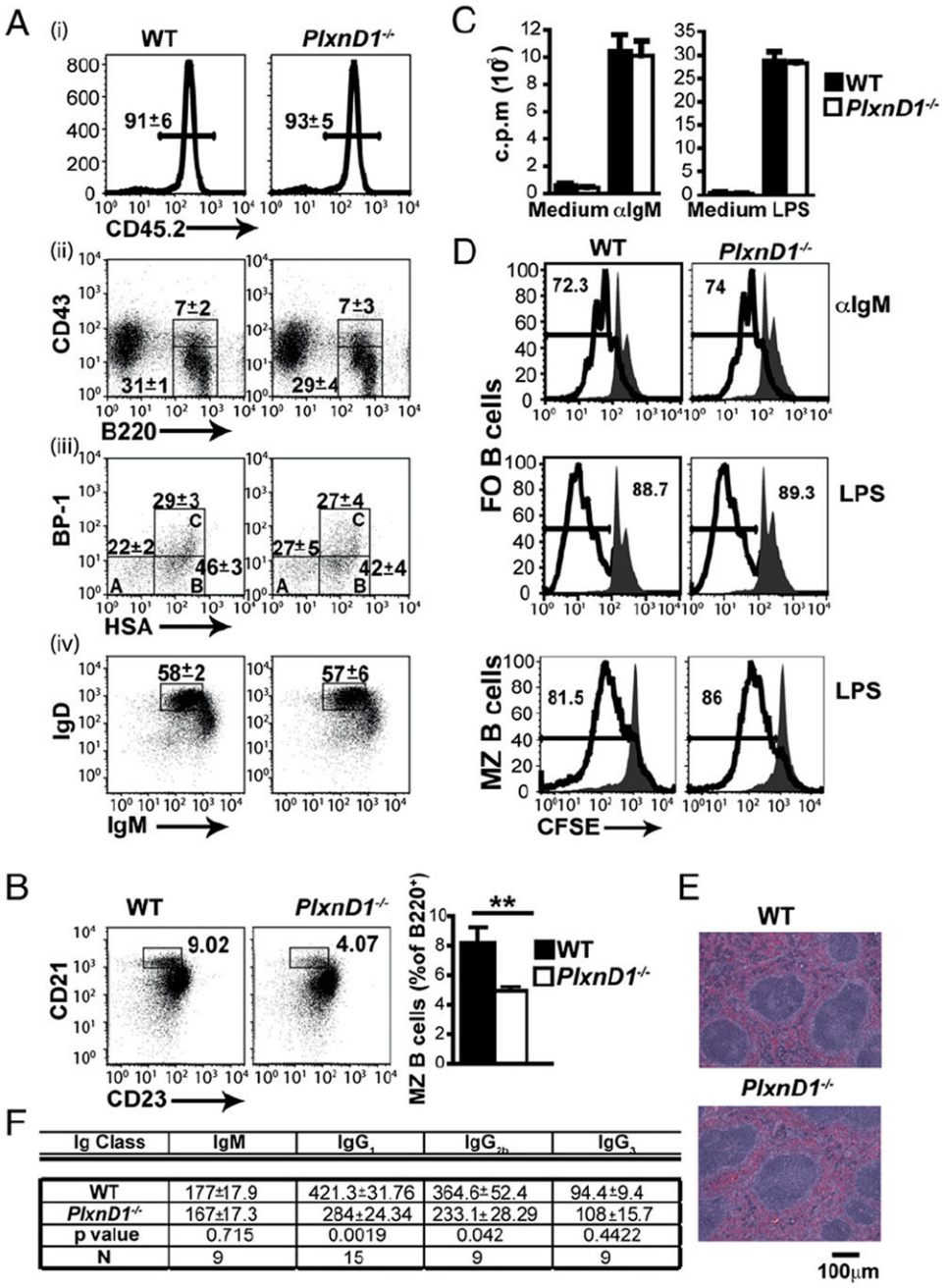

Ig Class	IgM	IgG_1	IgG_{2b}	IgG_3
WT	177±17.9	421.3±31.76	364.6±52.4	94.4±9.4
PlxnD1$^{-/-}$	167±17.3	284±24.34	233.1±28.29	108±15.7
p value	0.715	0.0019	0.042	0.4422
N	9	15	9	9

FIGURE 2.

Normal in vitro function exhibited by *PlxnD1*$^{-/-}$ B cells. *A*, Reconstitution of irradiated recipients with WT and *PlxnD1*$^{-/-}$ fetal liver cells. mAb to CD45.2 was used to label splenocytes and to determine the percentage of reconstitution. WT and *PlxnD1*$^{-/-}$ fetal liver cells reconstituted equally well (*i*). mAbs to B220 and CD43 (*ii*), and HSA and BP1 (*iii*) were used to determine the percentages of B cell progenitors in the BM using Hardy's fractionation (*ii, iii*). mAbs to B220, IgM, and IgD were used to determine the percentage of mature FO B cell population in the spleen (*iv*). Plots are pregated on live $CD45.2^+B220^+$ lymphocytes. Data are representative of 10 mice for each genotype. Mean percentage ± SEM is indicated for each cell type. *B*, mAbs to CD45.2, B220, CD21, and CD23 were used

to determine the percentage of MZ B cell populations in the spleen, WT (■), and *PlxnD1*$^{-/-}$ (□). Plots were pregated on B220^{+} splenocytes. Graph represents data pooled from nine mice in three different experiments. $^{**}p < 0.01$. *C*, Proliferation of B cells from mice reconstituted with *PlxnD1*$^{-/-}$ and WT fetal liver cells, as assessed by [^{3}H]thymidine uptake. WT (■) or *PlxnD1*$^{-/-}$ (□) FO B cells were cultured in the presence of 5 μg/ml anti-IgM or 5 μg/ml LPS for 48 h. Cells were pulsed with [^{3}H]thymidine for the last 8 h in culture to determine cell proliferation, and data are presented as cpm. $n = 9$ mice per group. Data are representative of three independent experiments. *D*, Proliferation of *PlxnD1*$^{-/-}$ and WT B cells, as assessed by CFSE dilution. Data are representative of three independent experiments. $n = 9$ mice per group. *E*, Splenic structure of mice reconstituted with *PlxnD1*$^{-/-}$ and WT fetal liver cells. H&E staining of 5-μm spleen cryosections was performed. Five spleens were analyzed for each genotype. *F*, Serum Ig levels in mice reconstituted with *PlxnD1*$^{-/-}$ and WT fetal liver cells. Data were pooled from three independent experiments. $n = 9$–14 mice per group.

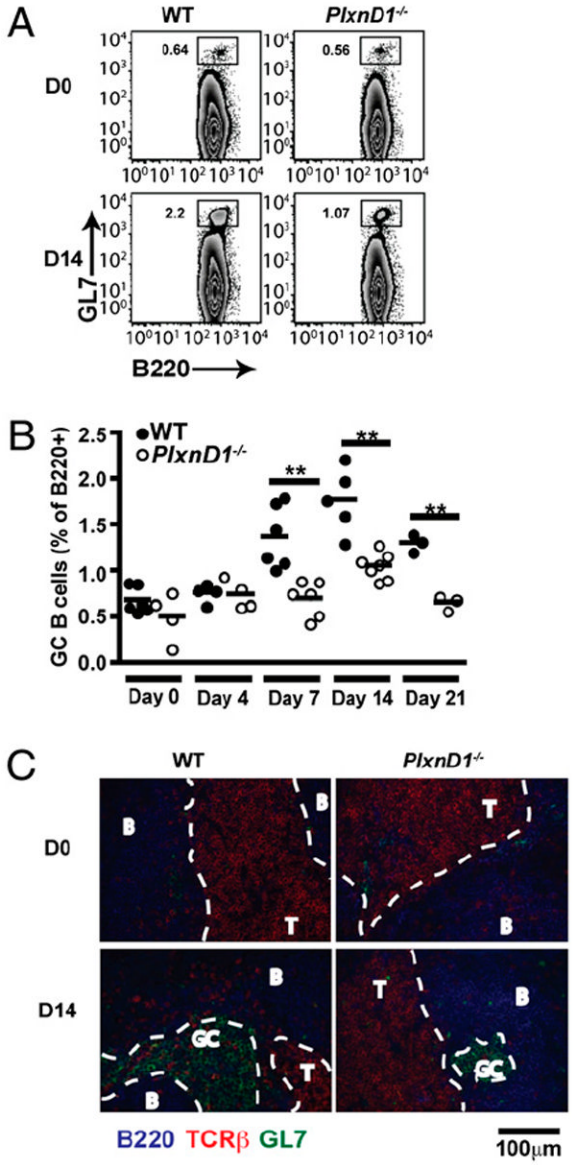

FIGURE 3.

Impaired GC response in *PlxnD1*$^{-/-}$ mice. *A*, Reduced frequency of GC B cells in mice reconstituted with *PlxnD1*$^{-/-}$ cells relative to those with WT cells, as measured by flow cytometry. Mice were immunized (i.p.) with 10 μg NP_{18}-CGG in alum and spleens were harvested at day 14 postimmunization. The percentage of B220^{high}GL-7^{high} B cells of total B220^{high} cells was determined by flow cytometry. *B*, Reduced frequency of GC B cells in *PlxnD1*$^{-/-}$ (○) mice relative to WT (●) mice. Quantification of GC B cells as measured by flow cytometry. The graph is representative of three independent experiments. Each point represents data from one mouse. Small horizontal bars indicate mean values. $^{**}p < 0.001$. *C*, Reduction of GC size in mice reconstituted with *PlxnD1*$^{-/-}$ cells relative to those with WT cells, as measured by histology. Sections (5 μm) of spleens from WT and *PlxnD1*$^{-/-}$ mice at day 14 postimmunization were labeled with B220–AF350 (blue), TCRβ–PE (red), and GL-7–FITC (green) Abs. FITC signal was amplified using anti–FITC-AF488 Ab. Images were acquired using a Zeiss Axiovert 200M confocal immunofluorescent microscope. Day 0 samples are shown as control. $n = 10$ mice per group.

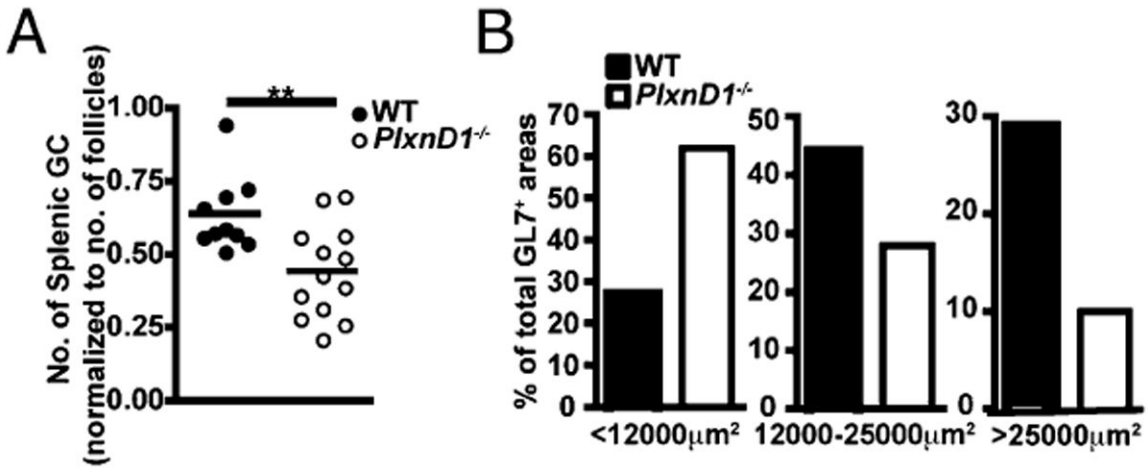

C

Genotype	No. GC analyzed	Median area	Mean area(±SEM) ***
WT	206	20449	23840±1247
PlxnD1$^{-/-}$	212	9676	14580±1026

FIGURE 4.

Decreased number and size of GCs in *PlxnD1*$^{-/-}$ mice. *A*, Reduced GC number in *PlxnD1*$^{-/-}$ (○) mice than WT (●). Number of GCs was counted using five to eight different 5-μm sections for each mouse spleen divided by the total number of B cell follicles. Each point represents data from one mouse. Data were pooled from three independent experiments. Small horizontal bars indicate mean values. $^{**}p < 0.001$. *B*, Reduced percentage of larger GC in mice reconstituted with *PlxnD1*$^{-/-}$ cells (□) compared with WT (■). GCs were divided into three groups, as follows: small (<12,000 μm^2), medium (12,000–25,000 μm^2), and large (>25,000 μm^2). The number of GCs in each group was divided by the total number of GCs and was presented as a percentage. More than 200 GCs were analyzed for each group. *C*, Reduced GC area in *PlxnD1*$^{-/-}$ mice. Area of individual GCs was determined 14 d postprimary NP-CGG immunization using ImageJ. Data are pooled from three independent experiments. $n = 13$. $^{***}p < 0.0001$.

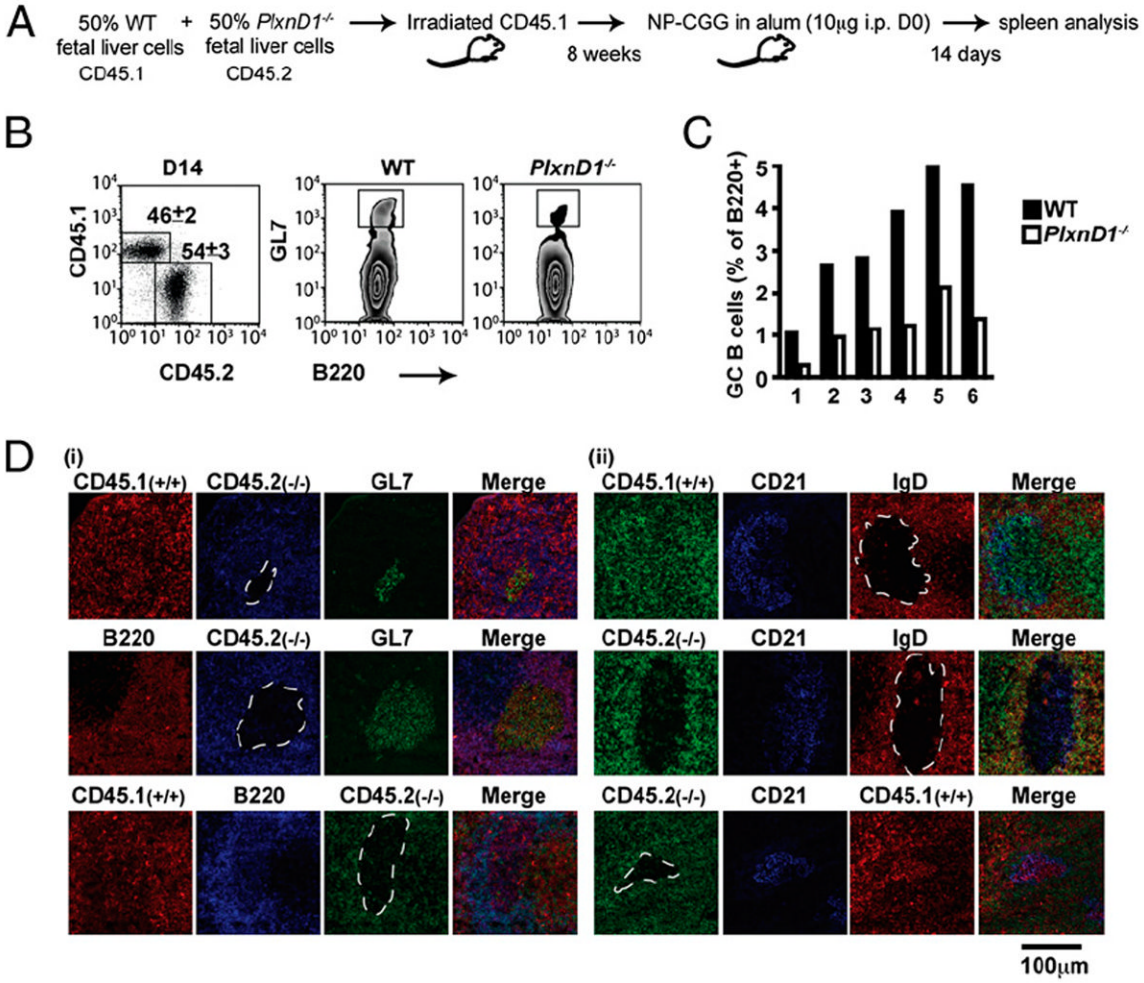

FIGURE 5.

PlxnD1$^{-/-}$ B cells participate in the GC reaction less efficiently than WT B cells. *A*, Schematic of experimental design. *B*, Reduced frequency of *PlxnD1*$^{-/-}$-derived GC B cells relative to those with WT cells, as measured by flow cytometry. Mice were immunized (i.p.) with NP-CGG in alum, and spleens were harvested at day 14 postimmunization. Percentage of FO B cell reconstitution was determined by flow cytometry using anti-B220, CD45.1, and CD45.2 Abs. The percentage of *PlxnD1*$^{-/-}$ CD45.2^{+}B220^{high}GL-7^{high} B cells of total B220^{high} cells was determined by flow cytometry and was reduced relative to the percentage of WT CD45.1^{+}B220^{high}GL-7^{high} controls. $n = 6$ mice per group. Mean ± SEM are presented for each genotype. Data were obtained in two separate experiments. *C*, Reduced frequency of GC B cells in *PlxnD1*$^{-/-}$ (□) B cells relative to WT (■) B cells. Quantification of GC B cells, as measured by flow cytometry. The graph is representative of two independent experiments. Each point represents data from one mouse. $p < 0.001$. *D*, Splenic sections from chimeric mice were stained with various combinations of CD45.1, CD45.2, GL-7, and B220 Abs to determine the presence of WT and *PlxnD1*$^{-/-}$ B cells in the GCs (*i*). Splenic sections from WT/*PlxnD1*$^{-/-}$ chimeric mice were stained with various combinations of CD45.1, CD45.2, IgD, and CD21 Abs to determine the presence of WT and *PlxnD1*$^{-/-}$ B cells in the GC light and dark zones (*ii*). Images were acquired using a Zeiss LSM 710 confocal immunofluorescent microscope. $n = 6$ mice per group.

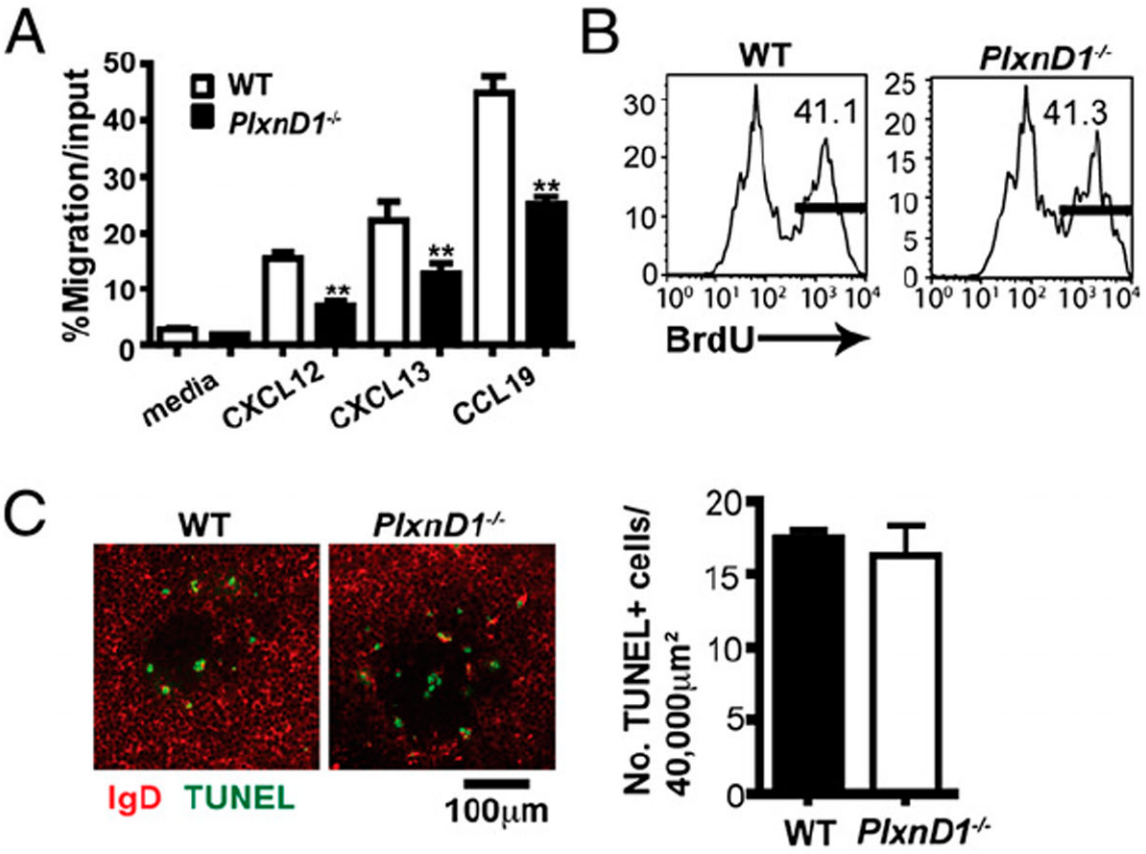

FIGURE 6.

Impaired in vitro migration of activated *PlxnD1*$^{-/-}$ B cells, but normal GC B cell proliferation and cell death. *A*, Purified WT (□) and *PlxnD1*$^{-/-}$ (■) FO B cells were activated in vitro, placed in the same well, and subjected to competitive in vitro migration assays in the presence of medium alone, CXCL12, CXCL13, and CCL19 (*A*). WT and *PlxnD1*$^{-/-}$ B cells were differentiated by CD45.1 and CD45.2 expression. Migrated cells were quantified by flow cytometry and are presented as percentage of total input cells. n = 6–7 mice per group. *B*, WT and *PlxnD1*$^{-/-}$ mice were immunized with NP-CGG. Ten days postimmunization, mice were injected i.p. with BrdU (1 mg/ml in PBS) and sacrificed 5 h later. Splenocytes were labeled with anti-IgM, IgD, B220, and BrdU Abs to distinguish GC B cells. BrdU incorporation is expressed as percentage of total GC B cells. Data are representative of four individual mice per group. *C*, Sections (5 μm) of spleens from WT and *PlxnD1*$^{-/-}$ mice at day 14 postimmunization were labeled with IgD–PE (red) and TUNEL (green) Abs. Images were acquired using a Zeiss Axiovert 200M confocal immunofluorescent microscope. TUNEL^{+} cells were quantitated for individual mice and pooled. n = 4 mice per group.

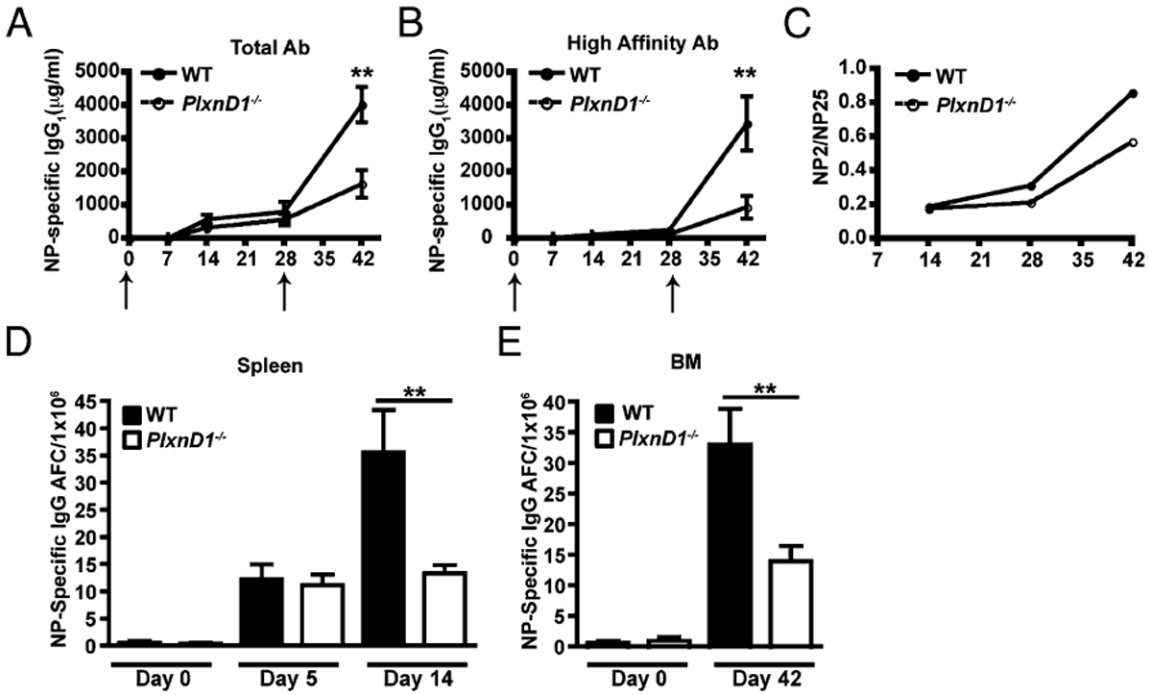

FIGURE 7.

Impaired secondary T_d immune response in *PlxnD1*$^{-/-}$ mice. *A* and *B*, Serum Ig levels after primary and secondary immunization in WT (solid line) and *PlxnD1*$^{-/-}$ (dotted line) mice. Mice were immunized (i.p.) with NP_{18}-CGG in alum and boosted at day 28 postprimary immunization. Serum was harvested at various time points. Data were pooled from three independent experiments. $^{**}p < 0.01$ and $n = 11$ mice per group. *C*, The ratio of NP2/NP25 was estimated as an indicator of affinity maturation. *D*, Ag-specific splenic AFC formation in mice reconstituted with WT (■) and *PlxnD1*$^{-/-}$ (□) fetal liver cells. Spleens were harvested at day 5 and 14 postimmunization. NP-specific IgG AFC were enumerated by ELISPOT. *E*, Ag-specific BM AFC formation in mice reconstituted with *PlxnD1*$^{-/-}$ and WT fetal liver cells. BM was harvested at day 14 postsecondary immunization. NP-specific IgG AFC were enumerated, as above. Data were pooled from three independent experiments. Mean ± SEM. $^{**}p < 0.01$ and $n = 10$ mice per group.